Inorganica Chimica Acta, *88* (1984) 153–160

Molecular and Crystal Structures of $[(Ph_3P)_2N][B_3H_7(NCS)]$ and $[(Ph_3P)_2N][B_3H_7(NCSe)]$; the Need for Low-Temperature X-Ray Crystallography

STEVEN J. ANDREWS and ALAN J. WELCH

Department of Chemistry, University of Edinburgh, West Mains Road, Edinburgh, EH9 3JJ, U.K.

Received January 21, 1984

Two ion pairs of $[(Ph_3P)_2N][B_3H_7(NCS)]$ crystallise in the centrosymmetric triclinic space group with a = *10.0206(16),* b = *10.9026(13) and* c = *17.482(3)* Å, α = *109.063(13),* β = *101.409(14) and* γ = *76.480(12)°* *at 185 ± 1 K. The isocyanate and isoselenocyanate analogues $[(Ph_3P)_2N][B_3H_7(NCO)]$ and $[(Ph_3P)_2N][B_3H_7(NCSe)]$ are isomorphous with* a = *9.839(4),* b = *11.199(3),* c = *17.408(5)* Å, α = *110.638(23),* β = *101.553(27),* γ = *79.019(24)° at 291 ± 2 K), and* a = *10.129(2),* b = *10.887(2),* c = *17.488(4)* Å, α = *108.835(15),* β = *101.286(19),* γ = *75.764(18)°* *(at 185 ± 1 K) respectively. Diffraction data were collected at both ambient and low temperatures for the (NCS) and (NCSe) analogues, and for both species analysis of room and low temperature data suggests different stereochemical arrangements of the borane hydrogen atoms; one edge- and one face-bridging H is suggested from the room temperature data sets, whilst the low temperature data reveal only one (edge-) bridging hydrogen atom for each compound. The latter data afford* R = *0.0471 for 5515 observed reflections (NCS) and* R = *0.0493 for 4888 reflections (NCSe).*

Introduction

There is substantial and continuing interest in the stereochemistries and reactivities of substituted derivatives of the octahydrotriborate anion $[B_3H_8]^-$. Previous structural studies of $[B_3H_7X]^{-n}$ have delineated two major structural classes; that containing a single B–H–B bridge, exemplified by X = CO, n = 0 [1], X = PR_3, n = 0 [2], and that containing two B–H–B bridges, as shown by $[B_3H_8]^-$ itself [3], and by [*trans*-1,2-$B_3H_6(Cl)_2]^-$ [4]. However, the hydrogen atoms in such compounds tend to be fluxional, consistent with n.m.r. spectra of derivatives [2, 5], and with very small energy differences between the alternative forms calculated at several levels of sophistication for $[B_3H_8]^-$ [6].

Recently, we have determined the molecular structure of $[(Ph_3P)_2N][B_3H_7(NCS)]$, **1**, at ambient temperature [7], and located and satisfactorily refined the (expected) μ_2-H and, additionally, a hydrogen atom bridging the triboron face. Such a result was unprecedented for a borane, although previous studies had demonstrated μ_3-H atoms in carbaboranes [8] and carbametallaboranes [9, 10]. In view of the expectation of unusual reactivity associated with such a system it was clearly of value to accurately define the positions of all atoms within the anion, and thus we have repeated the analysis at low temperature (LT).

To our consternation we found that the best interpretation of the LT data involved having only a single edge-bridging H atom in the anion. Wishing to obtain further accurate structural information with which to resolve this apparent anomaly, the isocyanate analogue $[(Ph_3P)_2N][B_3H_7(NCO)]$, **3**, was screened. Although shown to be isomorphous with the isothiocyanate it unfortunately yields crystals of too poor a quality to merit the collection of full diffraction data. The isomorphous isoselenocyanate $[(Ph_3P)_2N][B_3H_7(NCSe)]$, **2**, however, afforded good quality crystals, and therefore room temperature (RT) and LT data sets were collected from it. The results of all these structural studies are presented herein.

Experimental

The syntheses of $[(Ph_3P)_2N][B_3H_7(NCS)]$, **1**, and $[(Ph_3P)_2N][B_3H_7(NCO)]$, **3**, have been reported [5, 4], and the isoselenocyanate $[(Ph_3P)_2N][B_3H_7(NCSe)]$, **2**, is prepared by an analogous reaction to that affording **1** [11]. All species were recrystallised from dichloromethane.

Suitable single crystals of each compound were mounted on a thin glass fibre using LT epoxy-resin adhesive, and were screened for singularity and crystal quality by oscillation and Weissenberg X-ray photography. On the diffractometer 25 reflections, $28 < 2\theta < 30°$, were accurately centred and their setting angles used to determine, by least-squares, the accurate unit cell parameters and the orientation matrix. These data, together with other relevant

0020-1693/84/$3.00

© Elsevier Sequoia/Printed in Switzerland

TABLE I. Crystallographic Data and Data Collection Techniques.

Diffractometer	Enraf-Nonius CAD4				
Radiation	Mo-K$_\alpha$ ($\bar{\lambda}$ = 0.71069 A) Graphite monochromated				
Formula	$C_{37}H_{37}N_3P_2S_2$ 1 (RT)	$C_{37}H_{37}B_3N_2P_2S$ 1 (LT)	$C_{37}H_{37}B_3N_2P_2Se$ 2 (RT)	$C_{37}H_{37}B_3N_2P_2Se$ 2 (LT)	$C_{37}H_{37}B_3N_2OP_2$ 3
Temperature (K)	291	185	291	185	291
M	636.15		683.05		620.09
$F(000)$	668		704		652
Space Group	$P\bar{1}$	$P\bar{1}$	$P\bar{1}$	$P\bar{1}$	$P\bar{1}$
a (Å)	10.065(4)	10.0206(16)	10.163(3)	10.129(2)	9.839(4)
b (Å)	11.064(3)	10.9026(13)	11.044(4)	10.887(2)	11.199(3)
c (Å)	17.572(3)	17.482(3)	17.605(4)	17.488(4)	17.408(5)
α (deg)	109.228(19)	109.063(13)	109.125(25)	108.838(15)	110.638(23)
β (deg)	101.37(3)	101.409(14)	101.093(22)	101.286(19)	101.553(24)
γ (deg)	77.02(3)	76.480(12)	76.288(27)	75.764(18)	79.019(24)
V (A^3)	1784(1)	1740(1)	1799(1)	1755(1)	1744(1)
Z	2	2	2	2	2
ρ_c (g cm^{-3})	1.18	1.21	1.26	1.29	1.18
μ(Mo-K$_\alpha$) (cm^{-1})	1.69	1.73	11.00	11.28	1.51
Crystal size (mm)	0.5 × 0.3 × 0.1		0.6 × 0.4 × 0.2		0.6 × 0.2 × 0.05
Collection Range	$+h \pm k \pm l$, $2 \leqslant 2\theta \leqslant 50°$	$+h \pm k \pm l$, $2 \leqslant 2\theta \leqslant 54°$	$+h \pm k \pm l$, $2 \leqslant 2\theta \leqslant 50°$	$+h \pm k \pm l$, $2 \leqslant 2\theta \leqslant 50°$	
Scan type	w-2θ	w-2θ	w-2θ	w-2θ	
Scan width	0.85 + 0.35tanθ	0.85 + 0.35tanθ	0.85 + 0.35tanθ	0.85 + 0.35tanθ	
Max. Counting Time (s)	60	60	75	60	
X-Ray Exposure Time (h)	120	153	95	84	
No. Unique Data	6199	7565	6314	6151	
No. Data with $F_o \geqslant 2\sigma(F_o)$	4479	5515	4038	4888	
No. Parameters	355	355	355	355	
R	0.056	0.047	0.062	0.049	
Rw	0.080	0.058	0.079	0.068	
Largest Shift[a]	0.03	0.08	0.04	0.01	
Largest Peak (e A^{-3})[b]	0.37	0.35	0.67	0.85	

[a] Largest parameter shift in final refinement cycle. [b] Largest peak in final ΔF synthesis.

TABLE II. Fractional Coordinates of Refined Atoms for **1** (LT).

	x	y	z
P(1)[a]	0.99103(6)	0.78063(5)	0.71175(3)
P(2)	0.85348(6)	0.62493(6)	0.77415(3)
N(1)	0.87802(19)	0.73942(18)	0.74517(11)
C(12)	1.07630(16)	0.91473(14)	0.87088(8)
C(13)	1.13828[b]	1.01134	0.93203
C(14)	1.18977	1.10317	0.91153
C(15)	1.17928	1.09837	0.82987
C(16)	1.11729	1.00175	0.76872
C(11)	1.06580	0.90993	0.78922
C(22)	1.26516(13)	0.64477(12)	0.71423(7)
C(23)	1.36747	0.53608	0.68630
C(24)	1.33412	0.43132	0.61899
C(25)	1.19844	0.43525	0.57960
C(26)	1.09611	0.54394	0.60754
C(21)	1.12947	0.64870	0.67485
C(32)	0.76438(13)	0.87605(14)	0.61621(8)
C(33)	0.69576	0.91577	0.54824
C(34)	0.77093	0.91750	0.48954
C(35)	0.91471	0.87952	0.49880
C(36)	0.98332	0.83979	0.56678
C(31)	0.90816	0.83806	0.62548
C(42)	0.83502(15)	0.36054(13)	0.69778(7)
C(43)	0.79110	0.25707	0.63313
C(44)	0.71915	0.28094	0.56097
C(45)	0.69111	0.40828	0.55345
C(46)	0.73503	0.51175	0.61809
C(41)	0.80698	0.48788	0.69025
C(52)	0.65402(13)	0.60639(11)	0.85736(8)
C(53)	0.54058	0.65711	0.90073
C(54)	0.48328	0.79125	0.91859
C(55)	0.53943	0.87467	0.89309
C(56)	0.65287	0.82396	0.84972
C(51)	0.71016	0.68981	0.83185
C(62)	1.11138(14)	0.47544(14)	0.80038(7)
C(63)	1.23139	0.43533	0.84875
C(64)	1.23938	0.48107	0.93365
C(65)	1.12734	0.56692	0.97017
C(66)	1.00732	0.60703	0.92180
C(61)	0.99934	0.56129	0.83690
S(1)	0.40859(9)	0.85014(9)	0.65268(5)
C(1)	0.4613(3)	0.9866(3)	0.69909(16)
N(2)	0.5019(3)	1.0841(3)	0.73098(15)
B(1)	0.5714(4)	1.2036(3)	0.77202(23)
B(2)	0.7336(4)	1.1721(4)	0.8339(3)
B(3)	0.5843(4)	1.2487(3)	0.88195(22)
HB(11)	0.5172(11)	1.2973(11)	0.7626(9)
HB(12)	0.6733(11)	1.1875(11)	0.7414(9)
HB(21)	0.8119(11)	1.2358(11)	0.8437(10)
HB(22)	0.7719(11)	1.0570(11)	0.8123(9)
HB(31)	0.5670(11)	1.3587(11)	0.9122(9)
HB(32)	0.5080(11)	1.1960(11)	0.8881(9)
H('23)	0.7058(11)	1.1884(11)	0.9077(10)

[a] Atomic numbering scheme: C(i1)–C(i6) are phenyl carbons numbered cyclically, with C(i1) (i = 1–3) bound to P(1), and C(i1) (i = 4–6) bound to P(2). HB(ij) (j = 1, 2) are bound to B(i). H('23) bridges B(2) and B(3). [b] Phenyl rings refined as rigid bodies, hence errors in fractional coordinates are common.

crystallographic quantities, appear in Table I. Only for **1** and **2** were diffraction data collected, and in no case was significant crystal movement or decomposition detected by subsequent analysis of the orientation and intensity control reflections monitored throughout each experiment. All intensity data were corrected for Lorentz and polarisation effects but not for X-ray absorption. Only those reflections with $F_o \geqslant 2.0\sigma(F_o)$ were used to solve and refine the structures. For **1** and **2** both RT and LT data sets were measured, using, in each case, the same crystal.

Solution and Refinement

From the RT data sets for **1** and **2** structure solutions were achieved by automatic centrosymmetric direct methods (P and S/Se atoms) and an iterative combination of full-matrix least-squares refinement and difference Fourier syntheses (B, C, and N atoms). From the LT data sets satisfactory results were obtained by refinement of the appropriate (non-H containing) molecular skeletons given by the prior RT determinations.

The carbons of the phenyl groups were refined in regular planar hexagons, C–C = 1.395 Å, but with independent thermal parameters. Phenyl hydrogen atoms were set in idealised positions and allowed to ride on their respective carbons, with C–H = 1.08 Å and $U_H = 0.10$ (RT data) or $U_H = 0.05$ (LT data) Å^2. For each species six of the seven H atoms of the borane anion were readily located from a difference Fourier synthesis and were subsequently positionally refined. In **1** (RT) and **2** (RT) the seventh H-atom appeared as a μ_3-H, bridging the triboron face, and was successfully refined as such; in **1** (LT) and **2** (LT), however, the final H atom appeared as a semi-μ_2-H, bridging the B(1)–B(2) connectivity, again with successful positional refinement. In view of the greater accuracy of the LT *versus* RT analysis, taken in conjunction with the results of semi-empirical molecular orbital (MO) calculations (see Discussion), it must be concluded that the LT solutions are the more representative of the stereochemistry of these anions. Consequently only the refined positional parameters obtained from **1** (LT) and **2** (LT) are listed (Tables II and III, respectively).

Structure factors were weighted according to $w^{-1} = [\sigma^2(F_o) + x(F_o)^2]$ where x = 0.0021 [**1** (RT)], 0.000603 [**1** (LT)], 0.001945 [**2** (RT)], or 0.001884 [**2** (LT)]. In the final stages of refinement all non-hydrogen atoms were allowed anisotropic thermal motion leading to the discrepancy indices at convergence shown in Table I, where $R = \Sigma(\|F_o| - |F_c\|)/\Sigma|F_o|$, and $R_w = [\Sigma w(|F_o| - |F_c|)^2/\Sigma w(|F_o|)^2]^{1/2}$. Tables of final anisotropic temperature factors (Tables VIII and IX)*, and phenyl-H

---

*For footnote, please see overleaf.

TABLE III. Fractional Coordinates of Refined Atoms for 2 (LT).

	x	y	z
P(1)	−0.00700(8)	0.77821(8)	0.71259(5)
P(2)	−0.14311(8)	0.62342(8)	0.77471(4)
N(1)	−0.1188(3)	0.73829(25)	0.74585(15)
C(12)	0.26486(19)	0.63956(22)	0.71432(11)
C(13)	0.36678	0.53024	0.68569
C(14)	0.33423	0.42675	0.61808
C(15)	0.19976	0.43258	0.57909
C(16)	0.09784	0.54190	0.60772
C(11)	0.13039	0.64539	0.67533
C(22)	0.07688(24)	0.90966(20)	0.87120(12)
C(23)	0.13752	1.00577	0.93206
C(24)	0.18684	1.09829	0.91147
C(25)	0.17551	1.09471	0.83002
C(26)	0.11487	0.99861	0.76916
C(21)	0.06555	0.90608	0.78975
C(32)	−0.23105(18)	0.87798(20)	0.61811(11)
C(33)	−0.29904	0.91921	0.55049
C(34)	−0.22450	0.91985	0.49151
C(35)	−0.08199	0.87925	0.50014
C(36)	−0.01400	0.83802	0.56776
C(31)	−0.08853	0.83740	0.62675
C(42)	−0.26150(23)	0.51264(16)	0.61976(12)
C(43)	−0.30583	0.40993	0.55579
C(44)	−0.27768	0.28212	0.56347
C(45)	−0.20521	0.25702	0.63512
C(46)	−0.16088	0.35973	0.69909
C(41)	−0.18903	0.48755	0.69141
C(52)	−0.34120(21)	0.82469(16)	0.85170(12)
C(53)	−0.45453	0.87602	0.89468
C(54)	−0.51238	0.79203	0.91809
C(55)	−0.45690	0.65670	0.89851
C(56)	−0.34357	0.60536	0.85552
C(51)	−0.28572	0.68936	0.83212
C(62)	0.00956(21)	0.60280(24)	0.92182(12)
C(63)	0.12879	0.56163	0.96989
C(64)	0.24027	0.47482	0.93326
C(65)	0.23253	0.42918	0.84855
C(66)	0.11329	0.47034	0.80047
C(61)	0.00181	0.55716	0.83711
Se(1)	−0.58643(4)	0.84412(5)	0.65339(2)
C(1)	−0.5309(4)	0.9928(4)	0.70248(23)
N(2)	−0.4906(4)	1.0899(4)	0.73428(22)
B(1)	−0.4226(6)	1.2091(5)	0.7765(3)
B(2)	−0.2617(5)	1.1751(5)	0.8370(4)
B(3)	−0.4108(5)	1.2501(5)	0.8852(3)
HB(11)	−0.493(4)	1.309(4)	0.7682(22)
HB(12)	−0.349(4)	1.205(4)	0.7371(23)
HB(21)	−0.190(4)	1.230(4)	0.8375(22)
HB(22)	−0.231(4)	1.062(4)	0.8141(22)
HB(31)	−0.417(4)	1.361(4)	0.9150(22)
HB(32)	−0.488(4)	1.190(4)	0.8896(22)
H('23)	−0.281(4)	1.186(4)	0.9098(22)

TABLE IVa. Residuals from ΔF Synthesis for 1 (RT).

Peak	Residual (e $Å^{-3}$)	x	y	z	Assignment
1	0.646	0.7088	1.1767	0.9058	mu-H
2	0.477	0.8021	1.2406	0.8418	t-H
3	0.465	0.5152	1.1735	0.8833	t-H
4	0.398	0.5639	1.3605	0.9172	t-H
5	0.366	0.5208	1.3018	0.7675	t-H
6	0.363	0.5980	1.2792	0.8385	
7	0.351	0.7679	1.0740	0.7987	t-H
8	0.351	0.4837	1.0556	0.7854	
9	0.347	0.7020	0.1724	0.8236	
10	0.319	0.7032	0.3797	0.5578	
11	0.292	0.8780	0.4582	0.4003	
12	0.276	0.5687	0.2601	0.8779	
13	0.272	0.1536	1.0943	0.8651	
14	0.244	0.6407	1.2006	0.7209	
15	0.229	0.3479	0.4865	0.6623	

mu = μ_2-bridge; t = terminal

TABLE IVb. Residuals from ΔF Synthesis for 1 (LT).

Peak	Residual (e $Å^{-3}$)	x	y	z	Equivalent Peak in IVa
1	0.679	0.8040	1.2308	0.8423	2
2	0.588	0.7033	1.1998	0.9150	1
3	0.588	0.5170	1.1974	0.8988	3
4	0.522	0.5179	1.2953	0.7654	5
5	0.517	0.5704	1.3574	0.9116	4
6	0.512	0.7740	1.0651	0.8148	7
7	0.390	0.6767	1.1716	0.7464	14
8	0.365	0.9515	0.7997	0.6638	
9	0.340	0.3995	0.9331	0.6782	
10	0.330	1.1884	1.0566	0.9187	
11	0.299	0.5898	1.2380	0.8356	12
12	0.299	0.4794	1.0576	0.7843	8
13	0.289	0.9568	0.8601	0.5449	
14	0.289	1.1639	1.0967	0.8660	13
15	0.284	0.8532	0.6866	0.7366	

atom coordinates (Tables X and XI) for **1** (LT) and **2** (LT) are available as supplementary material. Comparisons of $10F_o$ *versus* $10F_c$ at the termination of refinement for all four determinations may also be obtained upon request. All crystallographic calculations were performed with the SHELX76 [12], XANADU [13], and XRAY 76 [14] programs

---

*Diffraction data for **2** were collected and the structure initially solved and refined using an alternative setting of the unit cell. Anisotropic temperature factors and structure factors have not been transformed, although positional parameters (Tables III and IVb) have been adjusted for consistency with those of **1**. The alternative cell (a′, b′, and c′) and the standard cell (a, b, and c) are related by the transformation

$$\begin{bmatrix} -1 & 0 & 0 \\ 0 & -1 & 0 \\ 0 & 1 & 1 \end{bmatrix} \times \begin{bmatrix} a' \\ b' \\ c' \end{bmatrix} = \begin{bmatrix} a \\ b \\ c \end{bmatrix}$$

TABLE V. Parameters used in EHMO Calculations for **1**

	Orbital	H_{ii} (eV)	ζ
S	3s	−20.00	1.817
	3p	−13.30	1.817
	3d	−8.00	1.500
B	2s	−15.20	1.300
	2p	−8.50	1.300
C	2s	−21.40	1.625
	2p	−11.40	1.625
N	2s	−26.00	1.950
	2p	−13.40	1.950
H	1s	−13.60	1.300

Distances and Angles (Å, degrees)

B–B	1.80
B–H(terminal)	1.10
B–H(bridge)	1.20
B–H(facial)	1.20
B–N	1.51
N–C	1.17
C–S	1.54
H(terminal)–B–H(terminal)	109.45
B–B–N	120.00
H(terminal)–B(1)–N(2)	101.11
H(terminal)–B(basal)–H(bridge)	100.61
B–N–C	180.00
N–C–S	180.00

Except, for face-bridging model:

H(terminal)–B(1)–B	120.00
H(terminal)–B(1)–N	109.45

implemented on the University of Edinburgh ICL 2972 computer, using inlaid neutral scattering factors for B, C, N, P, S and H [12], and, for Se, coefficients for an analytical approximation taken from 'International Tables for X-Ray Crystallography' [15].

Results and Discussion

Analysis of the RT diffraction data for **1** and **2** yield results that we believe to be misleading. Table IVa is a list of the 15 maximum residues in a ΔF synthesis computed with the RT data from **1** and using a $[(Ph_3P)_2N][B_3(NCS)]$ model ($R = 0.0621$). Peaks 1–5 and 7 correspond to one μ_2- and five terminal-H atoms. Peak 6 lies between 1.0 and 1.6 Å from all three boron atoms, and thus occupies an asymmetric μ_3-position. Table IVb is a similar list from the LT refinement of **1**. *There is no equivalent in IVb to peak 6 of IVa.* Rather, the 7th peak of IVb, whose equivalent in IV is peak 14, corresponds to a semi-μ_2-position. Thus, the molecular stereochemistries obtained from the RT and LT data for **1** are quite different if one assumes that maximal residual electron densities necessarily represent H-atom positions.

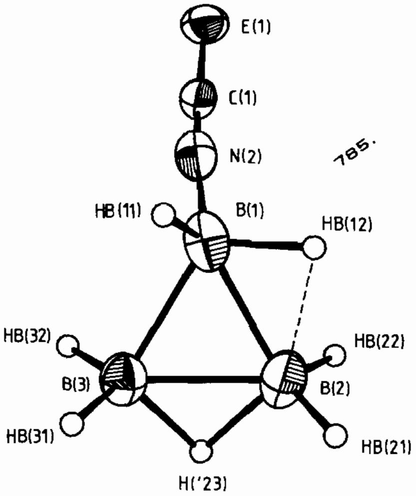

Fig. 1. Perspective view of the anions of 1 and 2, with atomic numbering scheme. Thermal ellipsoids are constructed at the 30% probability level (using data from **1** (LT)), except for H atoms which have an artificial radius of 0.1 Å for clarity. For **1** E = S, for **2** E = Se.

Broadly similar results were obtained from independent analysis of the RT and LT solutions of the isoselenocyanate **2**. Two crucial questions are (i) are these results mutually exclusive, and (ii) if so, which answer is the more reliable?

Although we cannot discount the possibility of a micro-scale phase change upon cooling **1** and **2** (and hence the possibility that the RT and LT solutions are not mutually inconsistent), equally we have no additional evidence to support such an unusual hypothesis. All other things being equal we would tend to have more confidence in the results of a low temperature analysis. In addition, extended Hückel (EH) MO calculations [16] on idealised models of $[B_3H_7(NCS)]^-$ with parameters specified in Table V show that the μ_2-H–μ_3-H model is destabilised by nearly 3 eV relative to the single μ_2-H model. Accordingly we believe that the more realistic results are those afforded by the LT determinations, and therefore emphasise the need for *low temperature* crystallographic studies of molecules of this type. All subsequent discussion refers only to the LT determinations.

Figure 1 presents a view of the anions of **1** and **2**, and Tables VI and VII list derived molecular parameters.

The boron triangle is markedly isosceles, with the bridged connectivity B(2)–B(3) *ca.* 0.02–0.04 Å the shortest. Actual B–B distances are very close to those of similar type observed in, for example, $[B_3H_6Cl_2]^-$ [4] and $[(B_3H_7NC)_2Ag]^-$ [17]. All terminal B–H bonds are of expected length, and

TABLE VI. Molecular Dimensions for **1** (LT).

(a) *Internuclear Distances* (Å)

P(1)–N(1)	1.5801(20)[a]	B(1)–B(3)	1.807(5)
P(1)–C(11)	1.7967(16)	B(1)–HB(11)	1.087(14)
P(1)–C(21)	1.7957(14)	B(1)–HB(12)	1.197(14)
P(1)–C(31)	1.7984(15)	B(2)–B(3)	1.760(5)
P(2)–N(1)	1.5752(20)	B(2)–HB(12)	1.660(14)
P(2)–C(41)	1.7957(15)	B(2)–HB(21)	1.119(14)
P(2)–C(51)	1.7923(14)	B(2)–HB(22)	1.178(14)
P(2)–C(61)	1.7916(15)	B(2)–H('23)	1.319(14)
S(1)–C(1)	1.600(3)	B(3)–HB(31)	1.128(14)
C(1)–N(2)	1.154(4)	B(3)–HB(32)	1.097(14)
N(2)–B(1)	1.520(5)	B(3)–H('23)	1.312(14)
B(1)–B(2)	1.793(6)		

(b) *Interbond Angles* (°)

N(1)–P(1)–C(11)	110.54(9)	B(3)–B(1)–HB(12)	119.1(7)
N(1)–P(1)–C(21)	114.83(9)	HB(11)–B(1)–HB(12)	100.4(10)
N(1)–P(1)–C(31)	108.11(9)	B(1)–B(2)–B(3)	61.13(22)
C(11)–P(1)–C(21)	108.05(7)	B(1)–B(2)–HB(21)	119.1(8)
C(11)–P(1)–C(31)	109.57(7)	B(1)–B(2)–HB(22)	105.9(7)
C(21)–P(1)–C(31)	105.56(7)	B(1)–B(2)–H('23)	107.2(6)
N(1)–P(2)–C(41)	112.51(9)	B(3)–B(2)–HB(21)	115.8(8)
N(1)–P(2)–C(51)	107.46(9)	B(3)–B(2)–HB(22)	123.8(7)
N(1)–P(2)–C(61)	113.93(9)	B(3)–B(2)–H('23)	47.8(6)
C(41)–P(2)–C(51)	106.89(7)	HB(21)–B(2)–HB(22)	117.2(10)
C(41)–P(2)–C(61)	107.36(7)	HB(21)–B(2)–H('23)	104.9(9)
C(51)–P(2)–C(61)	108.40(7)	HB(22)–B(2)–H('23)	100.7(9)
P(1)–N(1)–P(2)	141.43(14)	B(1)–B(3)–B(2)	60.36(22)
S(1)–C(1)–N(2)	178.1(3)	B(1)–B(3)–HB(31)	113.5(7)
C(1)–N(2)–B(1)	173.7(3)	B(1)–B(3)–HB(32)	100.1(7)
N(2)–B(1)–B(2)	114.7(3)	B(1)–B(3)–H('23)	106.8(6)
N(2)–B(1)–B(3)	111.7(3)	B(2)–B(3)–HB(31)	119.0(7)
N(2)–B(1)–HB(11)	117.6(8)	B(2)–B(3)–HB(32)	124.4(8)
N(2)–B(1)–HB(12)	108.5(7)	B(2)–B(3)–H('23)	48.2(6)
B(2)–B(1)–B(3)	58.51(21)	HB(31)–B(3)–HB(32)	116.4(10)
B(2)–B(1)–HB(11)	127.6(8)	HB(31)–B(3)–H('23)	112.6(9)
B(2)–B(1)–HB(12)	63.8(7)	HB(32)–B(3)–H('23)	106.2(9)
B(3)–B(1)–HB(11)	99.3(8)	B(2)–H('23)–B(3)	84.0(8)

[a] Estimated standard deviations, shown in parentheses throughout this paper, are right-adjusted to the least significant digit in the preceding number.

TABLE VII. Molecular Dimensions for **2** (LT).

(a) *Internuclear Distances* (Å)

P(1)–N(1)	1.573(3)	B(1)–B(3)	1.794(8)
P(1)–C(11)	1.7913(23)	B(1)–HB(11)	1.18(4)
P(1)–C(21)	1.7891(24)	B(1)–HB(12)	1.10(4)
P(1)–C(31)	1.7968(22)	B(2)–B(3)	1.763(8)
P(2)–N(1)	1.577(3)	B(2)–HB(12)	1.89(4)
P(2)–C(41)	1.7911(22)	B(2)–HB(21)	1.04(4)
P(2)–C(51)	1.7894(21)	B(2)–HB(22)	1.15(4)
P(2)–C(61)	1.7963(24)	B(2)–H('23)	1.29(4)
Se(1)–C(1)	1.742(4)	B(3)–HB(31)	1.15(4)
C(1)–N(2)	1.156(6)	B(3)–HB(32)	1.17(4)
N(2)–B(1)	1.524(7)	B(3)–H('23)	1.39(4)
B(1)–B(2)	1.788(8)		

(continued on facing page)

TABLE VII. *(continued)*

(b) *Interbond Angles* (°)

N(1)–P(1)–C(11)	115.11(13)	B(3)–B(1)–HB(12)	131.2(21)
N(1)–P(1)–C(21)	110.28(13)	HB(11)–B(1)–HB(12)	94.8(29)
N(1)–P(1)–C(31)	108.13(13)	B(1)–B(2)–B(3)	60.7(3)
C(11)–P(1)–C(21)	108.28(11)	B(1)–B(2)–HB(21)	115.1(22)
C(11)–P(1)–C(31)	105.32(10)	B(1)–B(2)–HB(22)	102.7(20)
C(21)–P(1)–C(31)	109.51(11)	B(1)–B(2)–H('23)	110.2(18)
N(1)–P(2)–C(41)	112.70(13)	B(3)–B(2)–HB(21)	121.6(22)
N(1)–P(2)–C(51)	107.41(12)	B(3)–B(2)–HB(22)	120.3(20)
N(1)–P(2)–C(61)	113.95(13)	B(3)–B(2)–H('23)	51.2(18)
C(41)–P(2)–C(51)	106.54(10)	HB(21)–B(2)–HB(22)	117.2(30)
C(41)–P(2)–C(61)	107.31(11)	HB(21)–B(2)–H('23)	111.6(28)
C(51)–P(2)–C(61)	108.62(11)	HB(22)–B(2)–H('23)	98.5(27)
P(1)–N(1)–P(2)	141.31(19)	B(1)–B(3)–B(2)	60.3(3)
Se(1)–C(1)–N(2)	178.1(4)	B(1)–B(3)–HB(31)	111.2(20)
C(1)–N(2)–B(1)	174.1(4)	B(1)–B(3)–HB(32)	99.3(20)
N(2)–B(1)–B(2)	114.9(4)	B(1)–B(3)–H('23)	105.2(17)
N(2)–B(1)–B(3)	111.5(4)	B(2)–B(3)–HB(31)	112.1(20)
N(2)–B(1)–HB(11)	112.7(19)	B(2)–B(3)–HB(32)	122.6(20)
N(2)–B(1)–HB(12)	106.2(21)	B(2)–B(3)–H('23)	46.5(16)
B(2)–B(1)–B(3)	59.0(3)	HB(31)–B(3)–HB(32)	125.2(28)
B(2)–B(1)–HB(11)	132.1(19)	HB(31)–B(3)–H('23)	107.7(26)
B(2)–B(1)–HB(12)	77.7(21)	HB(32)–B(3)–H('23)	106.5(25)
B(3)–B(1)–HB(11)	98.1(19)	B(2)–H('23)–B(3)	82.4(22)

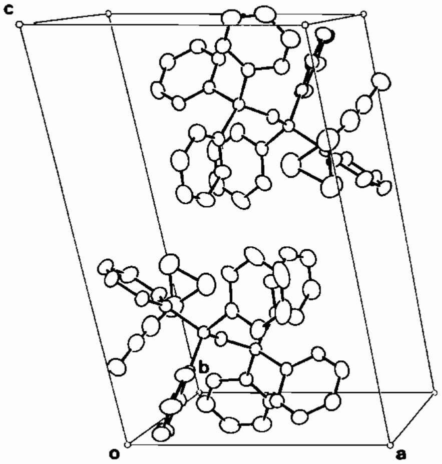

Fig. 2. Packing diagram. For the sake of clarity no H atoms are included.

there is, in addition, a weak, semi-bridging interaction between B(2) and HB(12), 1.660(14) Å in **1** and 1.89(4) Å in **2**. By comparison, B(3)–HB(11) is 2.255(17) Å in **1** and 2.28(3) Å in **2**. The BNCS and BNCSe fragments are nearly linear and have quite normal interatomic distances.

There are no close contacts between ion pairs. The $[(Ph_3P)_2N]^+$ cations are bent at N (*ca.* 143°). The conformations of these ions (best viewed along the P···P vector) are closely equivalent and very nearly staggered, mean torsion angles [18] being 55.36° (**1**) and 55.33° (**2**). There are no quasi-graphitic interactions of phenyl rings either within or between cations. Figure 2 presents a view of the crystal packing.

Acknowledgements

We thank Dr. J. H. Morris and his colleagues at the University of Strathclyde for preparing the crystalline samples, Borax Research Ltd. for a CASE studentship (S.J.A.) and the SERC for funds with which to purchase the diffractometer. Helpful discussion with Dr. R. O. Gould is gratefully acknowledged.

Supplementary Material Available

Tables VIII and IX: thermal parameters for **1** (LT) and **2** (LT) (2 pages); Tables X and XI: phenyl hydrogen atom coordinates for **1** (LT) and **2** (LT) (2 pages); Tables of $10F_o$ *versus* $10F_c$ for **1** (RT) (27 pages), **1** (LT) (33 pages), **2** (RT) (24 pages), and **2** (LT) (29 pages). This material is available from A. J. W. on request.

References

1 J. D. Glore, J. W. Rathke and R. Schaeffer, *Inorg. Chem., 12*, 2175 (1973).

2 V. L. Bishop and G. Kodama, *Inorg. Chem.*, *20*, 2724 (1981).

3 C. R. Peters and C. E. Nordman, *J. Am. Chem. Soc.*, *82*, 5758 (1960).

4 M. Arunchaiya, J. H. Morris, S. J. Andrews, D. A. Welch and A. J. Welch, *J. Chem. Soc., Dalton Trans.*, in press.

5 G. B. Jacobsen and J. H. Morris, *Inorg. Chim. Acta*, *59*, 207 (1982).

6 M. L. McKee and W. N. Lipscomb, *Inorg. Chem.*, *21*, 2846 (1982).

7 S. J. Andrews, A. J. Welch, G. B. Jacobsen and J. H. Morris, *J. Chem. Soc., Chem. Commun.*, 749 (1983).

8 E. A. McNeil and F. R. Scholer, *Inorg. Chem.*, *14*, 1081 (1975).

9 J. R. Pipal and R. N. Grimes, *Inorg. Chem.*, *18*, 252 (1979).

10 J. R. Pipal and R. N. Grimes, *Inorg. Chem.*, *18*, 263 (1979).

11 D. G. Meina and J. H. Morris, to be published.

12 G. M. Sheldrick, 'SHELX76', University Chemical Laboratory, Cambridge, England, 1976.

13 G. M. Sheldrick and P. Roberts, 'XANADU', University Chemical Laboratory, Cambridge, England, 1976.

14 'XRAY76', Technical Report TR-446, Computer Science Centre, University of Maryland, U.S.A., 1976.

15 'International Tables for X-Ray Crystallography', Kynoch Press, Birmingham, England, 1974, Vol. 4.

16 J. Howell, A. Rossi, D. Wallace, K. Haraki and R. Hoffmann, 'ICON8', *Quantum Chemistry Program Exchange*, *10*, 344 (1977).

17 S. J. Andrews and A. J. Welch, to be published.

18 C. Glidewell and D. C. Liles, *J. Organometal. Chem.*, *212*, 291 (1981).